https://doi.org/10.2352/ISSN.2470-1173.2018.16.COLOR-362

Comparative Study Of Biorthogonal Wavelets Accuracy In Demosaicing Algorithm Based On Wavelet Analysis Of Luminance Component

Norbert Hounsou; University of Abomey-Calavi, Institut de Mathématiques et de Sciences Physiques, Dangbo, Bénin.
Amadou T. SANDA MAHAMA ; University of Abomey-Calavi, Institut de Mathématiques et de Sciences Physiques, Dangbo, Bénin.
Pierre Gouton; University of Burgundy, Laboratoire Le2i; Dijon, France.
Jean-Baptiste Thomas; Norwegian Colour and Visual Computing Laboratory, NTNU, Norway.
.

Abstract

Critical issues in demosaicing are visual artifacts appearing in reconstructed images. Many algorithms have been proposed to overcome this problem. In this work, we have performed a comparative study of some conventional and recent color image demosaicing algorithms and identified experimentally the one that gives good results. From our investigation, algorithm based on wavelets analysis of the luminance component, is the best. Bi-orthogonal wavelets are recommended to be used in this algorithm. We then experiment famous bi-orthogonal wavelets to identify the best one. We conclude that Mallat's bi-orthogonal wavelets give the best reconstruction results according to CPSNR and FSIMc measures.

Introduction

Most popular digital cameras use a color filter array to sample a single chromatic value per spatial position. This process is called mosaicing. Bayer filter is the most used color filter array [1]. To estimate the full resolution color image with its three components, an interpolation algorithm is needed. Number of algorithms have been developed, but they all generate a certain degree visual artifacts such as blurring, introduction of false colors, aliasing, zipper effect, etc.

Demosaicing algorithms are numerous [2], going from the simple ones acting in each channel to determine the missing value, to more sophisticated ones which exploit the spatial and/or spectral correlation of pixels within a color. The performance of a demosaicing algorithm is measured in the ability of this one to reconstruct the color image with the less possible artifacts. Therefore, objective assessment of the reconstruction algorithms is done using measures such as the CPSNR [3] and the FSIMc [3, 4].

In this paper, using the Bayer color filter array and images of the Kodak and IMAX databases, we compare in table 1 and table 2 from top to down Demosaicing with directional filtering and a posteriori decision [5], Highly effective iterative demosaicing using Weighted-Edge and Color-Difference Interpolations [6], Exploitation of Inter-color Correlation for Color image demosaicking [7], Demosaicing based on Wavelet Analysis of the Luminance Component [8], Bilinear interpolation [13], Adaptive Residual Interpolation for color image demosaicking [9], Minimized-Laplacian Residual Interpolation for color image demosaicking [10], Residual Interpolation for color image demosaicking [11] and, Beyond Color Difference: residual interpolation for color image demosaicking [12].

In table 1, we compare nine demosaicing algorithms using Kodak database images. Ten images of Kodak database have been used for the experiment. Table 1 shows CPNSR measured in decibels (dB) and FSIMc measures of the reconstructed images. The best performances are bolded. Demosaicing algorithm based on the wavelets analysis of luminance component outperforms in a reasonably good time.

Table 2 shows the same measures but on ten images of IMAX database. It is difficult to elect the best algorithm based on these two metrics. The algorithm in [7] has the best CPSNR and the one in [9] the best FSIMc.

Due to the inconstancy of the performances in the IMAX database, we only take into account the results in table 1. Therefore the so-called algorithm Demosaicing based on wavelet analysis of luminance component have been elected. We then investigate the more suitable bi-orthogonal wavelets. Experiments lead to results and discussion for decision making.

Table 1: Comparison results of nine demosaicing algorithms with Kodak database

Algorithm	CPSNR	FSIMc	Δt(s)
DDFPD [5]	38.809	0.9987	1.89
WECDI [6]	37.44	0.9720	1.50
ICC [7]	41.63	0.9984	1.51
WALC [8]	**42.72**	**0.9988**	2.38
BI [13]	36.02	0.9795	**1.22**
BCD [12]	38.491	0.9986	3.32
ARI [9]	39.211	**0.9988**	38.70
MLRI [10]	38.946	0.9987	2.55

Table 2: Comparison results of nine demosaicing algorithms with IMAX database

Algorithm	CPSNR	FSIMc	Δt(s)
DDFPD [5]	36.06	0.9978	2.32
WECDI [6]	36.35	09655	**1.71**
ICC [7]	**40.54**	0.9983	1.73
WALC [8]	39.27	0.9977	3.41
BI [13]	39.94	0.9862	1.37
BCD [12]	38.11	0.9984	3.75
ARI [9]	38.18	**0.9987**	44.16
MLRI [10]	37.89	0.9984	2.59
RI [11]	37.71	0.9983	2.32

Demosaicing based on wavelet analysis of the luminance component (WALC)

This technique based on directional filtering uses new approach to localize details information in the image [8]. Edges directions are estimated using the luminance component and wavelets transforms give more accurate results. The algorithm is composed of different steps presented as follows:

Step1: Luminance estimation $\hat{L}$(x,y) as follows :

$$\begin{aligned} I_{CFA}(x,y) = \frac{1}{4}[R_0(x,y) + 2G_0(x,y) + B_0(x,y)] \\ + \frac{1}{4}[B_0(x,y) - R_0(x,y)](\cos \pi x \\ - \cos \pi y) \\ + \frac{1}{4}[-R_0(x,y) + 2G_0(x,y) \\ - B_0(x,y)](\cos \pi x \cos \pi y) \end{aligned} \quad (1)$$

In formula (1), the first term is the luminance component and the others, the chrominance component.

Step2: The estimated luminance component $\hat{L}$(x,y) is decomposed into horizontal $\hat{L}_{HL}$(x,y) and vertical components $\hat{L}_{LH}$(x,y) using low-pass and high-pass wavelet filter bank respectively.

Step3: Energy of the components $\hat{L}_{LH}$(x,y) et $\hat{L}_{HL}$(x,y) is processed e_{LH}(x,y) and e_{HL}(x,y) respectively. These energy values are used to determine two edge direction classifiers:

$$W_h x,y) = \frac{F * e_{HL}(x,y)}{F * e_{HL(x,y)} + F * e_{LH}(x,y)} \quad (2)$$

$$W_v x,y) = \frac{F * e_{LH}(x,y)}{F * e_{HL(x,y)} + F * e_{LH}(x,y)} \quad (3)$$

Step4: These classifiers are used to estimate green component.

$$\hat{G}(x,y) = w_h(x,y)\hat{G}_h(x,y) + w_v(x,y)\hat{G}_v(x,y) \quad (4)$$

Step5: Bilinear algorithm is used to estimate red and blue component at the green places. Red components at the blue places are estimated as follows :

$$\begin{aligned} \hat{\mathrm{R}}(\mathrm{x},\mathrm{y}) = \mathrm{B}(\mathrm{x},\mathrm{y}) + \frac{\mathrm{w_h}(\mathrm{x},\mathrm{y})}{2}(\hat{\mathrm{D}}_{\mathrm{RB}}(\mathrm{x}-1,\mathrm{y}) \\ + \hat{\mathrm{D}}_{\mathrm{RB}}(\mathrm{x}+1,\mathrm{y})) \\ + \frac{\mathrm{w_v}(\mathrm{x},\mathrm{y})}{2}(\hat{\mathrm{D}}_{\mathrm{RB}}(\mathrm{x},\mathrm{y}-1) \\ + \hat{\mathrm{D}}_{\mathrm{RB}}(\mathrm{x},\mathrm{y}-1)) \end{aligned} \quad (5)$$

Investigation on the biorthogonal wavelets

In [8] Cohen-Daubechie-Fauveau bi-orthogonal wavelets is used to decompose the estimated luminance component. In [18] authors show that bi-orthogonal wavelets under certain conditions ensure perfect image reconstruction and examples of bi-orthogonal filter banks that fit these conditions have been proposed.

Mallat's biorthogonal wavelet

It is a B-spline non symmetric wavelet [17]. In the first type of this wavelets, only the frequency response of an arbitrary filter have been given by Mallat. L.Shuguang Liu[15] has later proposed the second type of this wavelets and the filter bank H, G and K. The coefficients of these filters are obtained as follows :

$$H(w) = \begin{cases} e^{\frac{iw}{2}}(\cos(w/2))^m , & m = 2n-1, n \in Z^+ \\ \cos^m\left(\frac{w}{2}\right), & m = 2n, \quad n \in Z^+ \end{cases} \quad (7)$$

$$G(w) = \begin{cases} 4ie^{\frac{iw}{2}}\sin\left(\frac{w}{2}\right), & the\ 1^{st}\ kind\ wavelet \\ -16sin^2\left(\frac{w}{2}\right), & the\ 2^{nd}\ kind\ wavelet \end{cases} \quad (8)$$

(7) gives coefficients of the low-pass filter and (8) those of the high-pass filter.

The relation between K, L and H, G is shown as :

$$K(w) = \frac{1 - |H(w)|^2}{G(w)} \quad (9)$$

$$L(w) = \frac{1 + |H(w)|^2}{2} \quad (10)$$

See [13] for the details.

Biorthogonal wavelet proposed by Villasenor

Scale wavelets ϕ_A(x) and ϕ_S(x) have been proposed in [16]. For these scale wavelets, we have their corresponding mother functions Ψ_A(x) et Ψ_S (x).

$$\phi_A(x) = \sum_n 2^{\frac{1}{2}} h_0(n)\phi_A(2x-n) \quad (11)$$

$$\phi_s(x) = \sum_n 2^{\frac{1}{2}} g_0(n)\phi_s(2x-n) \quad (12)$$

The corresponding mother wavelets ΨA(x) and Ψ_S (x) are defined based on the scale functions and their filter coefficients:

$$\psi_A(x) = \sum_n 2^{\frac{1}{2}} h_1(n)\phi_A(2x-n) \quad (13)$$

$$\psi_s(x) = \sum_n 2^{\frac{1}{2}} g_1(n)\phi_s(2x-n) \quad (14)$$

For details, see [16].

Biorthogonal wavelet proposed by Vitterli and Herley

These wavelets filters are regular and with linear phase. In [17] authors show that under fairly conditions, bi-orthogonal wavelets synthesis filter ensure a perfect signal reconstruction. The filter bank coefficients they proposed and that we use are available in [17].

Biorthogonal wavelets proposed by Cohen-Daubechi-Fauvea(CDF)

The CDF wavelet is one of the widely used wavelet in image processing field in particular in image compression [18]. This wavelet is used in JPEG 2000. CDF bi-orthogonal wavelet is flexible and his filter bank length is short.

Experiments and results

Ten images picked from Kodak and IMAX databases have been used. Kodak database images are of format 768 x 512. In the case of Mallat's wavelets, orders 3 and 4 have been chosen for our experiments.

Figure 1: Ten images picked from Kodak database (first line) and IMAX database (second line) used in our experiments numbered form 1 to 10.

Table 3: Reconstruction performances using Mallat's first type order 3 wavelets filter

Image	CPSNR	FSIMc
1	40.86	**0.9990**
2	38.14	0.9985
3	**40.04**	**0.9991**
4	**36.95**	**0.9984**
5	38.19	**0.9987**
6	**33.38**	**0.9962**
7	32.97	**0.9973**
8	**38.09**	**0.9985**
9	**36.82**	**0.9977**
10	33.83	0.9976

Table 4: reconstruction performance using Mallat's first type order 4 wavelets filter

Image	CPSNR	FSIMc
1	40.35	0.9989
2	37.51	0.9983
3	39.98	**0.9991**
4	36.68	0.9982
5	37.93	0.9986
6	33.32	**0.9962**
7	32.87	0.9972
8	38.05	0.9984
9	36.78	**0.9977**
10	36.60	0.9974

Table 5: Reconstruction performance using Mallat's second type order 3 wavelets filter

Image	CPSNR	FSIMc
1	**41.07**	**0.9990**
2	**38.26**	**0.9986**
3	39.82	**0.9991**
4	36.89	**0.9984**
5	**38.35**	**0.9987**
6	33.22	0.9961
7	32.88	0.9972
8	38.05	**0.9985**
9	36.70	0.9976
10	**36.62**	0.9975

Table 6: Reconstruction performance using Mallat's second type order 4 filter

Image	CPSNR	FSIMc
1	41.02	**0.9990**
2	38.23	**0.9986**
3	40.00	**0.9991**
4	36.82	0.9983
5	38.26	**0.9987**
6	33.34	**0.9962**
7	**33.04**	**0.9973**
8	38.07	**0.9985**
9	36.76	0.9976
10	33.73	**0.9981**

Table 7: Reconstruction performance using Vitterly–Herley wavelets filter

Image	CPSNR	FSIMc
1	36.06	0.9977
2	34.63	0.9969
3	37.36	0.9984
4	35.03	0.9975
5	34.99	0.9977
6	32.17	0.9949
7	31.52	0.9959
8	37.52	0.9983
9	36.16	0.9973
10	32.36	0.9961

Table 8: Reconstruction performance using Cohen–Daubechie-Fauveau wavelets filter

Image	CPSNR	FSIMc
1	37.36	0.9981
2	34.86	0.9971
3	37.78	0.9985
4	35.45	0.9976
5	35.34	0.9978
6	32.18	0.9948
7	31.98	0.9962
8	37.44	0.9982
9	36.26	0.9973
10	32.30	0.9959

Table 9: Reconstruction performance using Vilasenor wavelets filter

Image	CPSNR	FSIMc
1	37.07	0.9980
2	37.63	0.9984
3	37.36	0.9983
4	34.93	0.9975
5	35.34	0.9978
6	32.18	0.9948
7	31.98	0.9962
8	37.44	0.9982
9	36.26	0.9973
10	32.30	0.9959

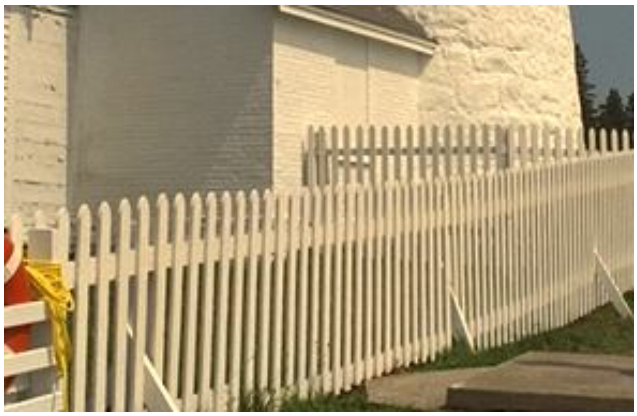

Figure 2. Close-up on the aliasing part of the original lighthouse image

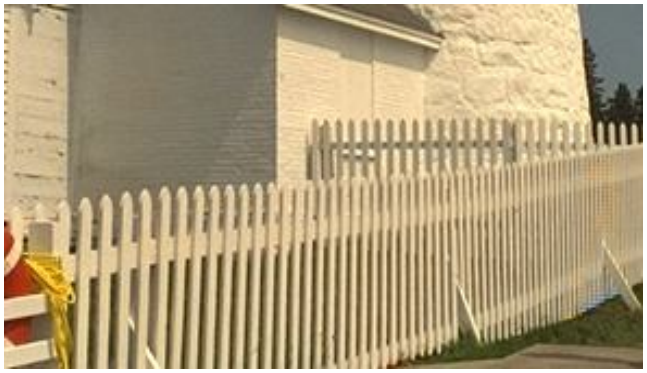

Figure 3 . Close-up on the aliasing part of the reconstructed lighthouse image using first type order 3 Mallat's wavelet

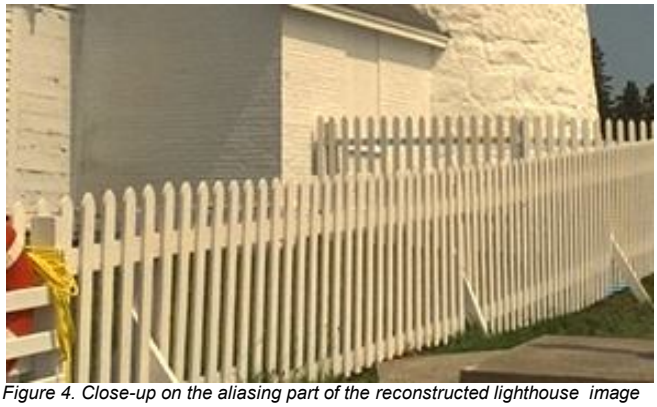

Figure 4. Close-up on the aliasing part of the reconstructed lighthouse image using first type order 4 Mallat's wavelet

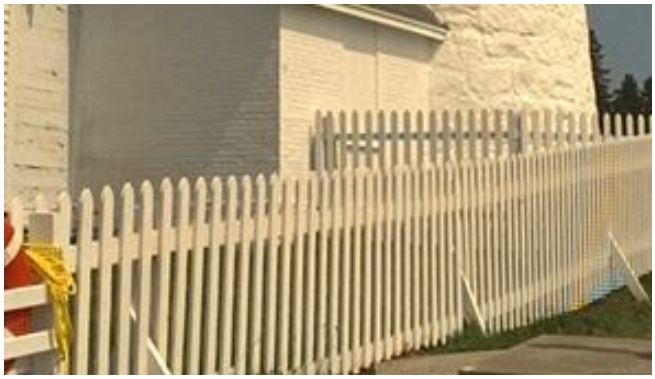

Figure 5. Close-up on the aliasing part of the reconstructed lighthouse image using second type order 3 Mallat's wavelet

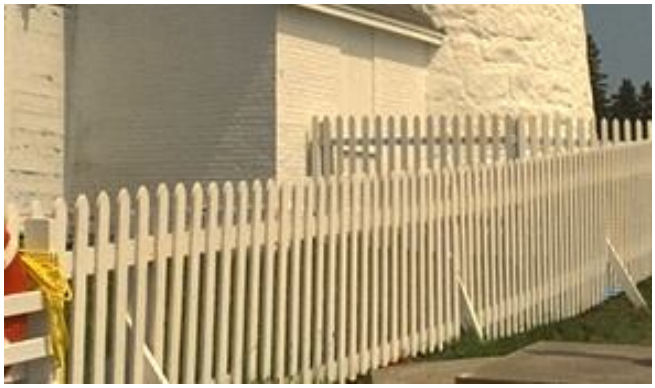

Figure 4. Close-up on the aliasing part of the reconstructed lighthouse image using second type order 4 Mallat's wavelet

Discussion

Reconstructed images have been evaluated comparing them to the original one. The objectives metrics CPSNR and the FSIMc are used for this evaluation. CPSNR and FSIMc values obtained from the comparison of each image to the original one are recorded in table 3 to 9, each table presenting results of the different wavelets. For each image, the best scores are bolded.

According to results depicted in the tables above, all the wavelets give good FSIMc values generally more than 0.990 as well as

CPSNR values generally more than 30. Nevertheless, Mallat's wavelets give the best reconstruction results.

Conclusion

In this paper we have reviewed some recent demosaicing algorihms. The comparison of their reconstruction accuracy shows that the one based on wavelets analysis of luminance component outperforms. This algorithm uses bi-orthogonal wavelets. According to our experiments, we have identified Mallat's wavelets as the one that give the best reconstruction results. In further works, we will assess this algorithm in the multispectral images context in order to compare it with the ones proposed in this area like Linear Minimum Mean Square error in [19].

References

[1] B. Bayer, "Color imaging array", United States patent 3,971,065, 1976.

[2] D. Alleyson, "30 ans de demosaicage - 30 years of demosaicing,", GRETSI 2004, vol. 21, pp. 561–581, 2004.

[3] P. Mohammadi, A. Ebrahimi-Moghadam, & S. Shirani, "Subjective and objective quality assessment of image: A survey.", arXiv preprint arXiv:1406.7799, 2014.

[4] L. Zhang, L. Zhang, X. Mou, & D. Zhang "FSIM: A feature similarity index for image quality assessment", IEEE transactions on Image Processing, 20(8), 2378-2386, 2011.

[5] D. Menon, S. Andriani, & G. Calvagno", Demosaicing with directional filtering and a posteriori decision", IEEE Transactions on Image Processing, vol. 16, 132-141, 2007.

[6] C. Y. Su, "Highly effective iterative demosaicing using weighted-edge and color-difference interpolations", IEEE Transactions on Consumer Electronics, vol. 52, no 2, p. 639-645, 2006.

[7] S. P. Jaiswal, O. C. Au, V. Jakhetiya, Y. Yuan, & H. Yang, "Exploitation of inter-color correlation for color image demosaicking'', IEEE International Conference on Image Processing (ICIP), Paris, France, 2014.

[8] D. Menon, and G. Calvagno, "Demosaicing based on wavelet analysis of the luminance component.", International Conference on Image Processing, IEEE. Vol. 2., San Antonio, TX, USA, 2007.

[9] J. F. Hamilton, and J. E. James Adams, "Adaptive color plan interpolation in single sensor color electronic camera", U.S. Patent No. 5,629,734. 13 May 1997.

[10] D. Kiku, Y. Monno, M. Tanaka, and M. Okutomi, ''Minimized-Laplacian Residual Interpolation for Color Image Demosaicking'', Proc. of SPIE-IS&T, Vol. 9023, p. 9023-9023-8, San Francisco, California, United States, 2014.

[11] D. Kiku, Y. Monno, M. Tanaka, & M. Okutomi, "Residual interpolation for color image demosaicking.", International Conference on Image Processing (ICIP), 20th IEEE, Melbourne, Australia, 2013.

[12] D. Kiku, Y. Monno, M. Tanaka, and M. Okutomi,''Beyond Color Difference: Residual Interpolation for Color Image Demosaicking'', IEEE Transactions on Image Processing , Vol. 25, p. 1288 – 1300, 2016.

[13] S. Gao, V. Gruev , "Bilinear and bicubic interpolation methods for division of focal plane polarimeters", Journal Optics Express**,** Vol. 19, pp. 26161-26173, 2011.

[14] Z. Zhao and H. Liao, '' Mallat wavelet filter coefficient calculation '', International Conference on Computational and Information Sciences, Shiyang, China, 2013.

[15] S. Liu, "Two Types of the S-pline Wavelets Based on Edge Detector", Basic sciences journal of textile universities, vol. 14, no 1, p. 66-71, 2001.

[16] J. D. Villasenor and J. Liao, ''Wavelet Filter Evaluation for Image Compression '', IEEE Transaction on image processing, vol 4. No 8, August 1995.

[17] M. Vitterli and C. Herley, '' Wavelets and Filter Banks: Theory and Design'', IEEE Transactions on signal processing, vol. 40, no 9, september 1992.

[18] A. Cohen, I. Daubechies, and J.-C. Feauveau, "Biorthogonal bases of compactly supported wavelets", Communications on pure and applied mathematics, 1992, vol. 45, no 5, p. 485-560.

[19] P. Amba, J. B. Thomas, & D. Alleysson, "N-LMMSE Demosaicing for Spectral Filter Arrays", Journal of Imaging Science and Technology, vol. 61, no 4, p. 40407-1-40407-11,2017.

Author Biography

Norbert Hounsou received MS degrees in physics (2006), and his MS degree in computer Sciences in 2014 from the University of Abomey-calavi. He is now pursuing a PhD program at University of Abomey-calavi.

Amadou T. Sanda Mahama received his MS degree in computer Sciences (2012) from University of Abomet-Calavi and his PhD (2016) from University of Burgundy (France) and University of Abomey-Calavi. His research focuses on color and multispectral imaging.

Professor, Pierre GOUTON. has obtained a PhD in Components, Signals and Systems at the University of Montpellier 2 (France), 1991. He has integrated the Department of Image Processing in the Laboratory of Electronics, Data-processing and Images. Since his main topic research carries on the segmentation of Images by Linear methods or None-linear mathematical morphology, classification), Color Science, Multispectral Images, Micro and Nano Sensor below.

Jean-Baptiste Thomas received his Bachelor in Applied Physics (2004) and his Master in Optics, Image and Vision (2006), both from University Jean Monnet in France. He received his PhD from University of Bourgogne (2009). He was researcher at the Gjovik University College and at the C2RMF. He is Associate Professor at University of Bourgogne. During 2015-16 he was 50% guest researcher at EPFL. His research focuses on color and multi-spectral imaging.